

# We are IntechOpen, the world's leading publisher of Open Access books Built by scientists, for scientists

6,900

Open access books available

186,000

International authors and editors

200M

Downloads

Our authors are among the

154

Countries delivered to

TOP 1%

most cited scientists

12.2%

Contributors from top 500 universities



WEB OF SCIENCE™

Selection of our books indexed in the Book Citation Index  
in Web of Science™ Core Collection (BKCI)

Interested in publishing with us?  
Contact [book.department@intechopen.com](mailto:book.department@intechopen.com)

Numbers displayed above are based on latest data collected.  
For more information visit [www.intechopen.com](http://www.intechopen.com)



# Morphology Development of Polymer Nanocomposites: Utilizing Interstratified Clay Minerals from Natural Systems

Kenji Tamura and Hirohisa Yamada  
*National Institute for Materials Science,  
Japan*

## 1. Introduction

Various nano-scale materials and an abundance of formulas that offer many potential benefits in our life and contribute to creating a sustainable society are latent in nature. For example, ubiquitous substances such as efflorescent soil minerals and rock contain various polymorphous nanomaterials like nano-balls, nano-tubes, and nano-sheets, which each have unique physicochemical properties including ion exchange, adsorption, colloidal characteristics, and swelling capabilities (van Olphen, 1977; Suzuki et al., 2001; Tamura & Nakazawa, 1996; Tamura et al., 1999, 2000). We benefit unknowingly from these materials in many ways. We can create innovative materials by learning their properties and mineral genesis.

Novel functional composite materials are being studied in our laboratory as a means to develop new engineering technologies for engineering ends. To improve various material properties such as strength, stiffness, corrosion resistance, surface finish, weight, and fatigue life, composites combine two or more substances on micro- and macroscopic scales to form useful materials. Of particular interest are the recently developed nanocomposites that consist of a polymer with a layered silicate, as they often exhibit remarkably improved mechanical and other properties when compared with pure polymers or conventional micro- and macro-composites (Kurauchi et al., 1991; Usuki et al., 1993; Maiti et al., 2001; Messersmith & Giannelis, 1994; Wang & Pinnavaia, 1998; Haraguchi & Takehisa, 2002; Yano, et al., 1997).

Generally, layered silicate-polymer nanocomposites are classified according to their levels of intercalation and exfoliation (Giannelis, 1992). At one end of this classification scheme are well ordered and stacked multilayers. These consist of intercalated polymer chains resident between host layers. At the other end are exfoliated silicate layers in a continuous polymer matrix. Some exfoliated clay-polymer nanocomposites have already been used in practical applications because of they are suitably rigid, strong, and exhibit barrier properties, whilst having far less silicate content than conventional composites that are filled with other minerals. Nanocomposite properties vary widely between the two extremes. The best results with respect to rigidity or barrier properties are obtained if the layered silicate is fully exfoliated into single layers with a thickness of about 1 nm. In spite of numerous

attempts reported during the past couple of decades, there has been no report of a nanocomposite with a rigorously controlled morphology.

Here, *morphology* is defined as the dispersion state of the clay components, called particles hereinafter, in the polymer matrix. Precise control of morphology is one of the most important factors in production of nanocomposites with desired properties. Although the control of morphology is still difficult, it can be a pivotal technique in studying how morphology, such as particle shape and size, affects the properties of nanocomposites. In this chapter, with respect to control of morphology, our attention was directed at the clay components to be dispersed and the number of layers of clay particles.

The following section highlights the various species and structures of layered silicates that are important when controlling the number of layers of dispersed silicate platelets. In particular, we focus strongly on interstratified clay minerals where two or more different individual component layers are stacked in various ways to make up a new structure, different from those of its constituents. These interstratified structures result from the strong similarity that exists between the layers of the different clay minerals, which are all composed of tetrahedral and octahedral sheets of hexagonal arrays of atoms, and from the distinct differences in the thickness of clay mineral layers. Later sections will explore specific types of nanocomposites that have been prepared using several types of interstratified clay minerals.

## 2. Structure of layered silicates

### 2.1 Tetrahedral sheet and octahedral sheet

The layers that form all phyllosilicates, and therefore clay minerals, are characterized by two-dimensional sheets with octahedral (**O**) or tetrahedral (**T**) configurations (Fig. 1). The octahedral (**O**) sheets are called dioctahedral if they contain two  $M^{3+}$  cations in six-fold coordination with  $O^{2-}$  or  $OH^-$ , in which case one of three cation sites remain vacant. If the octahedral sheets are made up of three  $M^{2+}$  cations coordinated with six  $O^{2-}$  or  $OH$  units, then all the cation sites are occupied by  $M^{2+}$  ions. The layers are then termed trioctahedral.

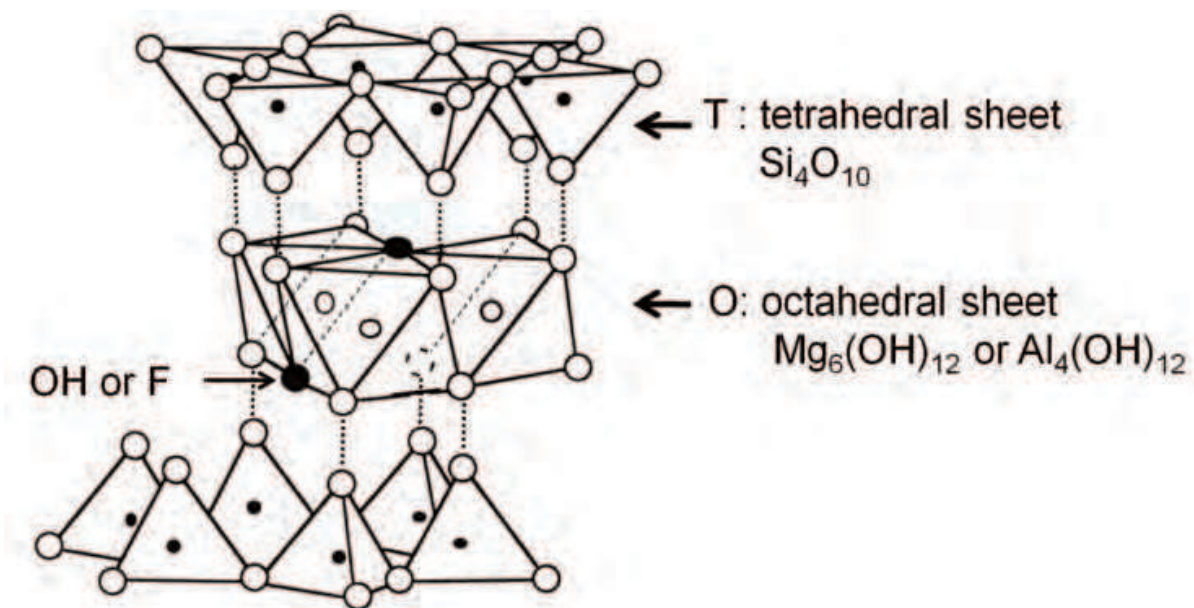


Fig. 1. Two-dimensional octahedral (O) and tetrahedral (T) sheets..

Tetrahedral (T) sheets are composed of cations organized in fourfold coordination with  $O^{2-}$  or  $OH^-$ . The dominant cation in such layers is usually  $Si^{4+}$ , but may also be  $Al^{3+}$ . The atomic arrangements of octahedral and tetrahedral layers are shown schematically in Fig. 1. The junction plane between the tetrahedral and octahedral sheets consists of shared apical oxygen atoms of the tetrahedrons and unshared hydroxyls (or fluorides) (Fig. 1). Typical layered clay minerals are listed in Table 1.

## 2.2 1:1 type layered silicates

Clays can be categorized depending on the way that tetrahedral and octahedral sheets are packaged into layers. If there is only one tetrahedral and one octahedral group in each layer the clay is known as a 1:1 TO layered silicate. The 1:1 TO layer type (kaolin-serpentine group) has one tetrahedral sheet, which shares corners with an octahedral sheet. The thickness of this two-sheet unit is about 0.7 nm (Fig. 2a). The kaolin group consists of 1:1 layer structures with the general composition of  $Al_2Si_2O_5(OH)_5$ . Kaolinite, dickite and nacrite are polytypes. Halloysite is a hydrated polymorph of kaolinite with curved layers and a basal spacing of about 1 nm due to hydration.

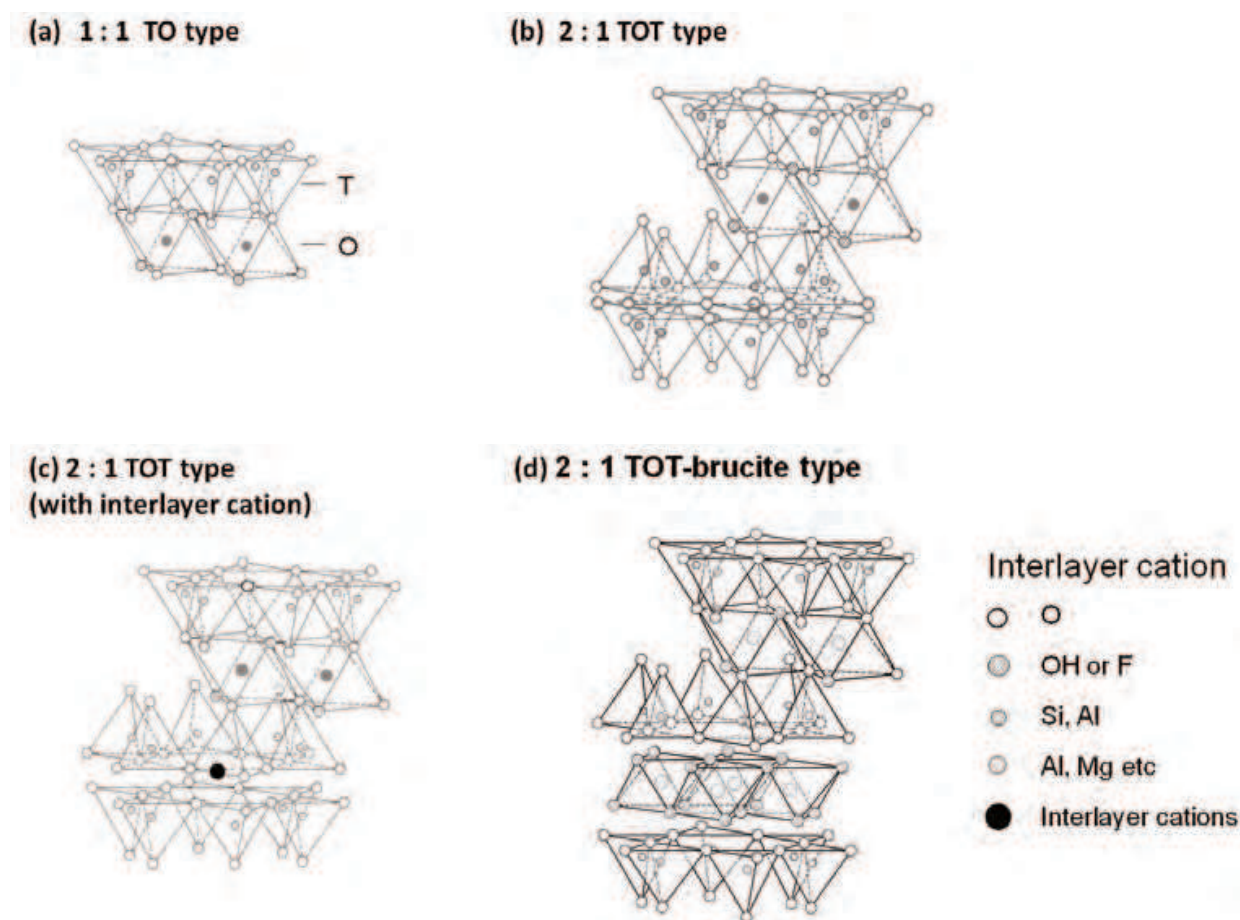


Fig. 2. Typical structures of layered silicates. (a) 1:1 layer type, kaolin-serpentine group; (b) 2:1 layered type, e.g. pyrophyllite or talc; (c) 2:1 layer type with interlayer cation (primarily K, Na, Ca, and Mg); and (d) 2:1 TOT layer type with brucite-like layer.

Layer Type	Group	Sub-group	Species	Chemical composition	
1 : 1 (x~0)	kaolin · serpentine	kaolin	kaolinite	$Al_2Si_2O_5(OH)_4$	
			dickite	↑	
			nacrite	↑	
		serpentine	halloisite	$Al_2Si_2O_5(OH)_4 \cdot 2H_2O$	
			chrysotile	$Mg_3Si_2O_5(OH)_4$	
			lizardite	↑	
		antigorite	$(Mg, Fe^{2+})_{2.0}Al(Si_{1.0}Al_{1.0})O_5(OH)_4 \cdot 2H_2O$		
2 : 1 (x~0) (x=0.2~0.6) (x=0.6~0.9) (x=0.6~1.0)	pyrophyllite · talc	pyrophyllite	pyrophyllite	$Al_2Si_4O_{10}(OH)_2$	
		talc	talc	$Mg_3Si_4O_{10}(OH)_2$	
	smectite	dioctahedral smectite	montmorillonite	$E_{0.33}(Al_{1.67}Mg_{0.33})Si_4O_{10}(OH)_2 \cdot nH_2O$	
			beidellite	$E_{0.33}Al_2(Si_{3.67}Al_{0.33})O_{10}(OH)_2 \cdot nH_2O$	
		trioctahedral smectite	saponite	$E_{0.33}Mg_3(Si_{3.67}Al_{0.33})O_{10}(OH)_2 \cdot nH_2O$	
			hectorite	$E_{0.33}(Mg_{2.67}Li_{0.33})Si_4O_{10}(OH)_2 \cdot nH_2O$	
			stevensite	$E_{0.33}Mg_{2.92}Si_4O_{10}(OH)_2 \cdot nH_2O$	
			sauconite	$E_{0.33}Zn_3(Si_{3.67}Al_{0.33})O_{10}(OH)_2 \cdot nH_2O$	
			vermiculite	dioctahedral vermiculite	$Mg_{2/x}Mg_3(Si_{4-x}Al)O_{10}(OH)_2 \cdot nH_2O$
		trioctahedral vermiculite	$Mg_{2/x}Al_2(Si_{4-x}Al)O_{10}(OH)_2 \cdot nH_2O$		
	mica	dioctahedral mica	muscovite	$KAl_2(Si_3Al)O_{10}(OH)_2$	
			paragonite	$NaAl_2(Si_3Al)O_{10}(OH)_2$	
			illite	$K_{0.75}Al_{1.75}R_{0.1}^{2+}(Si_{3.5}Al_{0.5})O_{10}(OH)_2$	
			celadonite	$KFe^{3+}(Mg, Fe^{2+})\square Si_4O_{10}(OH)_2$	
		trioctahedral mica	tobelite	$(NH_4)_{0.6}K_{0.2}Al_2(Si_{3.2}Al_{0.8})O_{10}(OH)_2$	
			phlogopite	$KMg_3(Si_3Al)O_{10}(OH)_2$	
			annite	$KFe^{2+}_3(Si_3Al)O_{10}(OH)_2$	
			lepidolite	$K(Li, Al)_3(Si, Al)_4O_{10}(F, OH)_2$	
	brittle mica	dioctahedral brittle mica	margarite	$CaAl_2(Si_2Al_2)O_{10}(OH)_2$	
			clintonite	$Ca(Mg, Al_3)(SiAl_3)O_{10}(OH)_2$	
		trioctahedral brittle mica	anandite	$Ba(Fe, Mg)_3(Si_3Fe^{3+})O_{10}(OH)_2$	
	2 : 1 : 1 (x variable)	chlorite	dioctahedral chlorite	donbassite	$Al_{4.27}(Si_{3.2}Al_{0.8})O_{10}(OH)_8$
			di-tri-octahedral chlorite	cookeite	$(LiAl_4)(Si_3Al)O_{10}(OH)_8$
sudoite				$(Al_{2.7}Mg_{2.3})(Si_{3.3}Al_{0.7})O_{10}(OH)_8$	
trioctahedral chlorite			clinocllore	$(Mg, Fe^{2+})_5Al(Si_3Al)O_{10}(OH)_8$	
			chamocite	$(Fe^{2+}, Mg, Fe^{3+})_5Al(Si_3Al)O_{10}(OH)_8$	

x : net layer charge per formula unit. E : exchangeable cation. □ : vacant.

Table 1. Classification of typical layered silicates related to clay minerals.

### 2.2 2:1 type layered silicate

The alternative, known as a 2:1 TOT layered silicate, has two tetrahedral sheets with the unshared vertices of each sheet pointing towards each other and forming each side of the octahedral sheet. The 2:1 TOT layer type with no interlayer cation, which includes pyrophyllite and talc, consists of two sheets of tetrahedra with an octahedral sheet sandwiched in between. These 2:1 layers are electrostatically neutral in the ideal case, with no interlayer ion present (Fig. 2b). The thickness of this 2:1 unit is about 0.91 nm to 0.94 nm. The 2:1 TOT layer type with interlayer cations consists mainly of the smectite, vermiculite, illite, and mica groups. It also contains 2:1 TOT layers, similar to Fig. 2b, which corresponds

to pyrophyllite and talc, but differs in that there is more significant isomorphous substitution, sufficient to raise the charge per unit cell. The net negative charge that arises from this is compensated for by interlayer cations (primarily K, Na, Ca and Mg) (Fig. 2c). The thickness of this platelet is about 1 nm.

### 2.3 2:1 type layered silicates (TOT-brucite)

Unlike other 2:1 clay minerals, in chlorites, the interlayer spaces between each 2:1 sandwich contain  $(Mg^{2+}, Fe^{3+})(OH)_6$ . This  $(Mg^{2+}, Fe^{3+})(OH)_6$  unit is more commonly referred to as the brucite-like layer (an octahedral sheet), due to its close resemblance to the mineral brucite  $(Mg(OH)_2)$ . Thus, chlorite's structure is as follows: T-O-T-brucite-... (Fig. 2d). The typical general formula is:  $(Mg,Fe)_3(Si,Al)_4O_{10}(OH)_2 \cdot (Mg,Fe)_3(OH)_6$  (see Table 1).

## 3. Interstratified clay minerals

### 3.1 Natural systems

Some natural clays consist of particles in which different types of silicate layers are stacked together (interstratification), and each type of silicate layer has swelling or non-swelling properties. These silicates are called interstratified clay minerals (Reynolds, 1980).

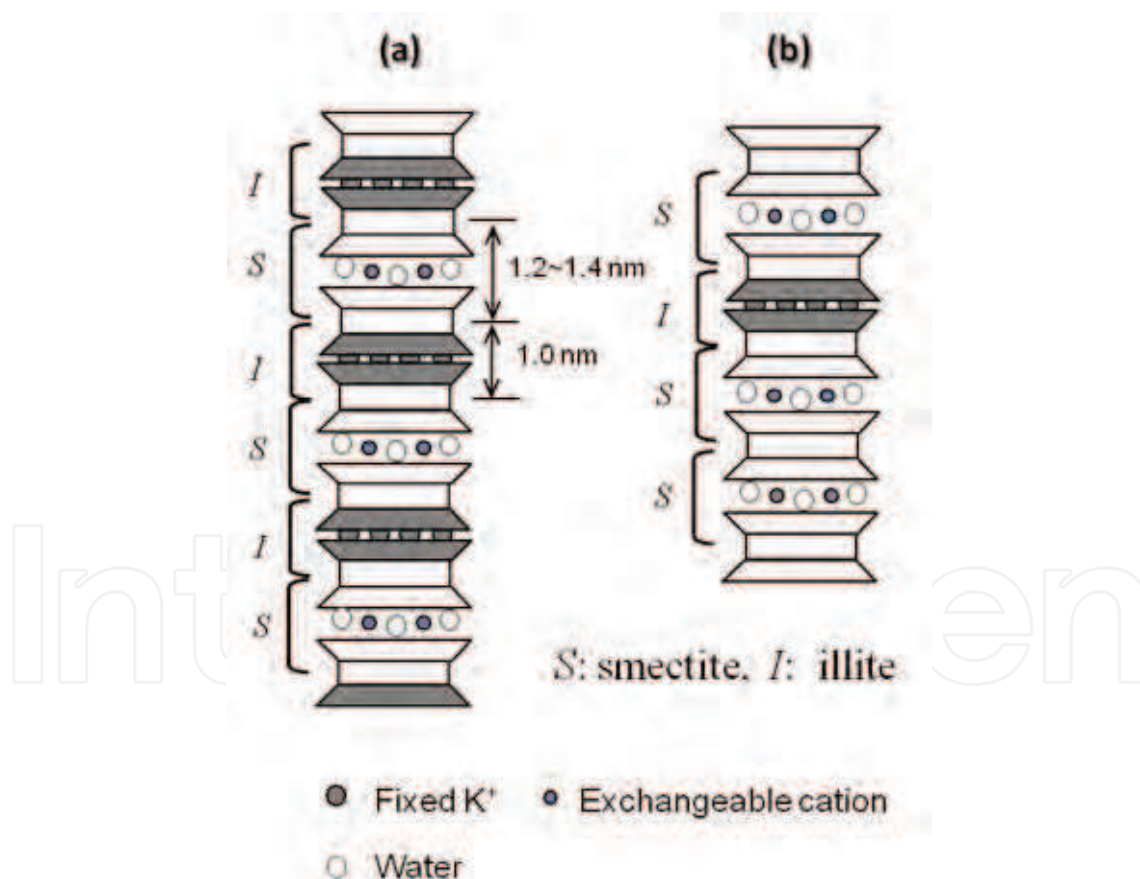


Fig. 3. Structures of interstratified clay minerals (illite/smectite system): (a) Regularly interstratified structure (1:1 type), and (b) Randomly interstratified structure.

Interstratified clay minerals can have ordered (or regular) mixed layer structures if different layers alternate along the  $c^*$  direction in a periodic pattern (e.g. the stacking of generic type

A and type B layers can be ...ABABAB... or ...AABAABAA...etc.). They can also have disordered (or irregular) mixed layer structures, wherein the stacking of type A and type B layers in the  $c^*$  direction is random (e.g. ...ABAAABABB...). These orderings are called regular or random, and are described by a Reichweite (R) ordering parameter (Jagodzinski, 1949a, 1949b, 1949c). For example, the regularly interstratified sequence of illite (I) and smectite (S) layers with a ratio of 1:1 refer to an ordering parameter R1. This type would be ordered in an ISIS fashion (Fig. 3a). On the other hand, Figure 3b shows random ordering which refer to R0. Figure 3 shows an example of interstratification between illite (I): anhydrous layers, with a periodicity of about 1.0 nm, and smectite (S): hydrated layers with a periodicity of about 1.2 nm to 1.4 nm. Interstratified clay minerals which are perfect R1 types often have individual names (Table 2). R1-ordered chlorite-smectite is known as corrensite, and R1 mica-smectite is rectorite. Special names are assigned to regularly alternating sequences of components present in a fixed ratio. Irregularly stacked structures are identified using the names of the two components, such as illite-smectite, smectite-chlorite and kaolinite-smectite. Typical interstratified clay minerals are listed in Table 3.

Mineral Name	Layer components	Regular alternation of layer types
Rectorite	Mica (di)/Smectite (di)	1 : 1
Tarasovite	Illite/Smectite (di)	3 : 1
Tosudite	Chlorite (di)/Smectite(di)	1 : 1
Brinrobertsite	Pyrophyllite/ Smectite (di)	1 : 1
Hydrobiotite	Mica(tri, Biotite) /Vermiculite(tri)	1 : 1
Corrensite	Chlorite(tri) / Vermiculite (tri)	1 : 1
	Chlorite(tri) / Smectite (tri)	1 : 1
Aliettite	Talc / Smectite (tri)	1 : 1
Kulkeite	Chlorite(tri) /Talc	1 : 1
Dozyite	Serpentine / Chlorite(tri)	1 : 1

Table 2. Regularly stacked, mixed clay minerals. di: dioctahedral, tri: trioctahedral.

In table 3, which lists the combinations between dioctahedral type layers and between trioctahedral type layers, there is only one combination between dioctahedral and trioctahedral type layers.

As shown in table 3, natural interstratified clay minerals mainly comprise combinations of two types of dioctahedral layers, or combinations of two types of trioctahedral layers. A combination of dioctahedral-type layer and trioctahedral-type layer is rarely found in nature. This is due to a larger misfit between the dioctahedral-type layer with the trioctahedral-type layer along the  $b^*$  axis. Each basic building block (layer) of interstratified clay minerals is generally assumed to possess the properties which are the same as the corresponding naturally-occurring mineral.

In order to define the basic building block (layer) of interstratified clay minerals, two possible structure models, which either have or do not have a center of symmetry placed between illite layers or smectite layers, are provided for regularly interstratified R1 I/S clay minerals. In the model which does not have the center of symmetry, an individual 2 : 1 layer in R1 I/S is always chemically homogeneous, consisting of either smectite or illite layer (Fig.4a). This model is referred to as non-polar 2:1 model. On the other hand, in the model having the center of symmetry (the symmetry is across the interlayer), an individual 2 : 1 layer in R1 I/S can be chemically homogeneous, containing a low charge smectite layer-like layer on one side and high charge illite-like layer on the other (Fig. 4b) which is referred to as polar 2:1 model. The polar model is supported by a number of NMR and XRD results (Altaner et al., 1988; Barron et al., 1985; Jakobsen et al., 1995; Plançon, 2004), and the first principle calculation (energy calculations) further reinforces the polar model (Olives et al., 2000; Stixrude & Peacor, 2002). The polar model is also consistent with the fundamental particle model by Nadeau et al.(1984) and the latest high resolution TEM result (Murakami et al., 2005).

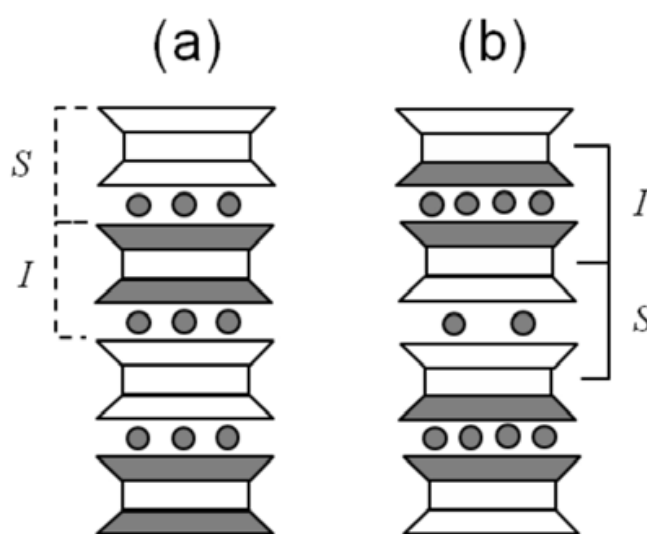


Fig. 4. Schematic of (a) non-polar and (b) polar models of the R1 I/S structure.

In the natural process of diagenesis, the transition of smectite to illite is an established axiom within the field of clay mineralogy. The formation of I/S minerals is actually affected not only by temperature, but also by other factors such as fluid chemistry, time, fluid/ rock (W/R) ratio during the formation of I/S minerals, and the chemical composition of the precursor materials (Altaner & Ylagan, 1997). Three of the most apparent variables driving the smectite-to-illite transition, called by some the illitization of smectite, are the time involved, the temperature, and the availability of interlayer K ions. As with all chemical reactions, time and temperature are inversely related (S´rodon´ & Eberl, 1984).

### 3.2 Synthesis of interstratified clay minerals

Many kinds of regularly interstratified clay minerals such as illite/smectite, mica/smectite, and chlorite/smectite have been found in nature. They are not, however, generally used as industrial materials because they are rare. Because of their scarcity, it is important to attempt to synthesize some interstratified clay minerals. Examples of previous research on synthesizing regularly interstratified clay minerals include studies on lizardite/saponite (smectite) and serpentine/smectite (Torii et al., 1998; Nagase et al., 2000).

	Combination	Layer components	
dioctahedral type - dioctahedral type	non-expandable layer/expandable layer	Illite - Smectite (di)	
		Illite - Vermiculite (di)	
		Mica (di) - Vermiculite (di)	
		Mica (di) - Smectite (di)	
		Glauconite - Smectite (di)	
		Chlorite (di) - Smectite (di)	
		Pyrophyllite - Smectite (di)	
		Pyrophyllite - Vermiculite (di)	
		Kaoline - Smectite (di)	
		Halloisite (7Å) - Halloisite (10Å)	
non-expandable layer/non-expandable layer	non-expandable layer/non-expandable layer	Chlorite (di) - Kaoline	
		Mica (di) - Pyrophyllite	
		Mica (di) - Chlorite (di)	
expandable layer/expandable layer	expandable layer/expandable layer	Vermiculite (di) - Smectite (di)	
		Smectite (di) - Smectite (di)	
trioctahedral type - trioctahedral type	non-expandable layer/expandable layer	Mica(tri, Biotite) - Vermiculite(tri)	
		Mica(Biotite) - Smectite(tri)	
		Chlorite(tri) - Vermiculite(tri)	
		Chlorite(tri) - Smectite(tri)	
		Talc - Smectite(tri)	
	non-expandable layer/non-expandable layer	non-expandable layer/non-expandable layer	Chlorite(tri) - Talc
			Serpentine - Chlorite(tri)
			Chlorite(tri) - Mica(Biotite)
	expandable layer/expandable layer	expandable layer/expandable layer	Vermiculite (tri) - Vermiculite (tri)
			Chlorite(tri) - Smectite (di)
dioctahedral type - trioctahedral type	non-expandable layer/expandable layer	Chlorite(tri) - Smectite (di)	

Table 3. Combinations of silicate layers in reported interstratified clay minerals.

In a previous study, we performed a series of hydrothermal experiments to determine the phase relationships of montmorillonite – stevensite and beidellite - saponite pseudo-binary joins (Yamada et al., 1999, 2010). Fig. 5 shows a three-component phase diagram of smectite with Si, Mg, and Al. Na is constant, and the figure shows the proportion of each element present in the smectites. Hydrothermal experiments were conducted using a rapid-quench type hydrothermal apparatus running at temperatures from 250 °C to 500 °C, with a constant pressure of 100 MPa and varying duration times. The time-temperature-phase change diagram in the both pseudo-binary join shows that immiscibility occurs between dioctahedral smectite (ex. montmorillonite-like smectite) and trioctahedral smectite (ex. stevensite-like smectite) below 400°C. It should be noted that interstratified clay minerals including rectorite-like interstratified layered silicate (composition I); a regularly interstratified chlorite/smectite (composition II); and a regularly interstratified talc/talc/smectite (composition III) were obtained at 350 °C (composition III), 450°C (composition I, II) in the intermediate chemical regions of these joins (Yamada et al., 1999, 2010). Of particular note was the montmorillonite-stevensite pseudo-binary join. On the

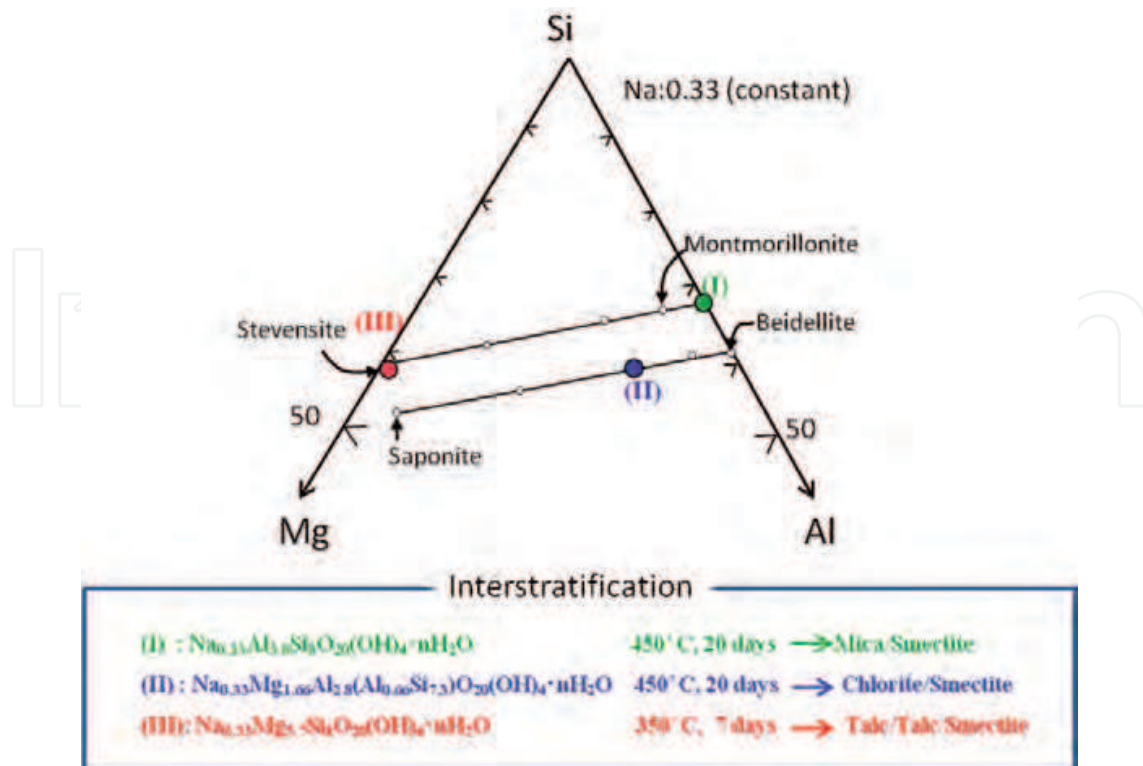


Fig. 5. A three-component phase diagram of smectites with Si, Mg, and Al. Na is constant, showing the proportion of each element present in the smectites.

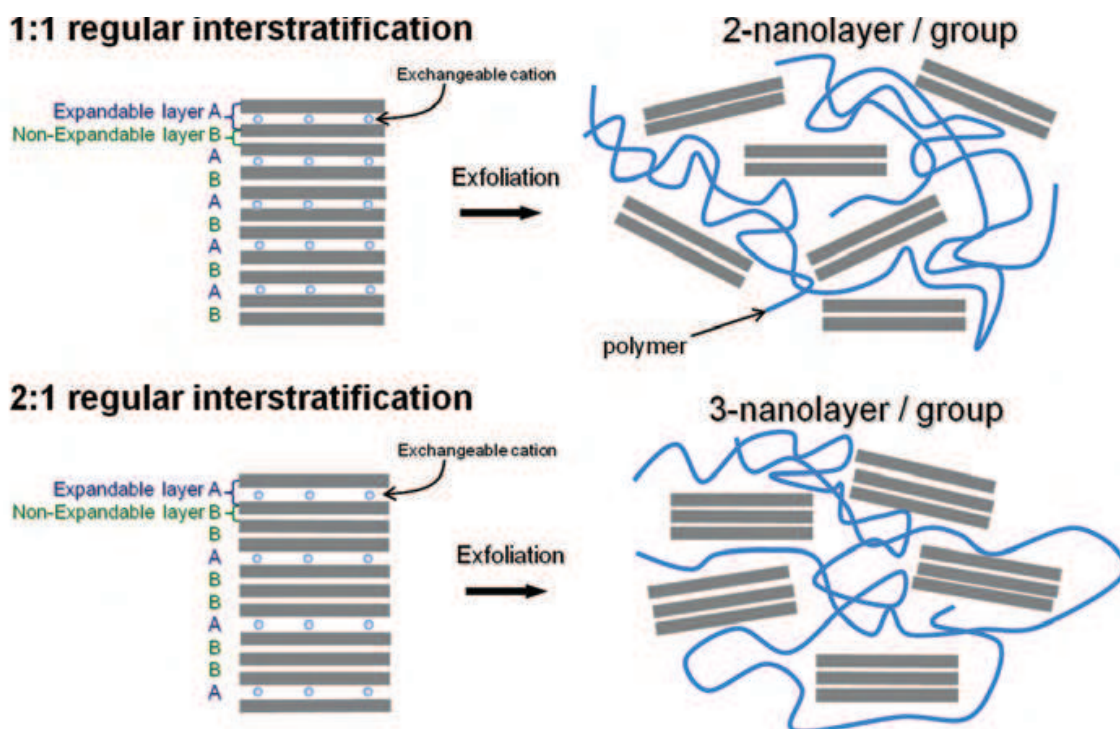


Fig. 6. Schematic diagram of the exfoliation process of regularly interstratified silicate layers: non-expandable layers are dispersed in a stacked condition after exfoliating the expandable layer.

stevensite side of this region, the trioctahedral smectite was found below 300°C, which transformed to stevensite and quartz with aging. Above 350°C, however, in the composition III, a regular interstratification was recognized, which was the regularly interstratified sequence of talc-like and smectite-like layers with a ratio of 2:1 (talc/talc/smectite) and a Reichweite (R) ordering parameter R2. The assemblage of regularly interstratified clay minerals was recognized in the intermediate chemical composition region of their joins. The following section explains the characterization of the synthesized interstratified clay minerals in more detail.

## 4. Interstratified clay minerals: polymer nanocomposites

### 4.1 Control of the number of layers

In order to achieve control of the number of layers, a layered silicate with two antagonistic properties, expandable and non-expandable characteristics, was prepared in each particle. Using these interstratified clay minerals with regularly alternating sequences of components, exfoliated nanolayers consisting of two or three layers per group could be dispersed in a polymer matrix (Fig. 6). The hydrophilic nature of these pristine clay minerals impedes their homogeneous dispersion in the polymer matrix. In most cases, the interlayer that has a expandable property must be organically modified. Unfortunately, it is difficult to obtain favorable materials having interstratified structures in ordered sequences because natural sources are impure and non-homogeneous, so it is important to create better-designed interstratified materials for inclusion in nanocomposites.

### 4.2 Morphology development of polymer nanocomposites

#### 4.2.1 Synthesized interstratified clay minerals

The time-temperature-phase change diagram described above showed that three types of regularly interstratified clay minerals occur above 350°C; product (I), a regularly interstratified mica/smectite (M/S), with a regular 1:1 layer type alternation, product (II), a regularly interstratified chlorite/smectite (C/S), which also has a 1 : 1 alternation, and product (III), a regularly interstratified talc/talc/smectite (T/T/S) with a 2:1 alternation (Fig. 5). The stacking structures were determined by examining different treatment samples using X-ray diffraction (XRD) measurement.

#### 4.2.2 Characterization of the synthesized interstratified clay minerals

To evaluate the layer stacking of the resulting material, two quenched samples were examined using XRD measurements. (1) The samples were oriented by sedimentation in water onto glass slides and then drying at room temperature. (2) An ethylene glycol (EG)-treated sample was prepared as follows: the oriented sample was placed in a sealed container with EG and then heated overnight at 60 °C. The phases encountered were identified using previously described criteria (Yamada et al., 1999, Tamura et al., 2008). Then, to prepare the nanocomposites, organically modified synthesized materials were made utilizing the ion-exchange reaction between exchangeable interlayer cations and octadecylamine (ODA) hydrochloride.

**Product (I)** By hydrothermal treatment of quenched glass with composition (I) at 450°C for 20 days, a layered silicate with a regularly interstratified structure was obtained (Tamura et al., 2009). Figure 7 shows the XRD patterns of (a) the pristine product (I), (b) an EG-treated sample and (c) an ODA treated sample. In the pristine product (I), a shoulder is observed at

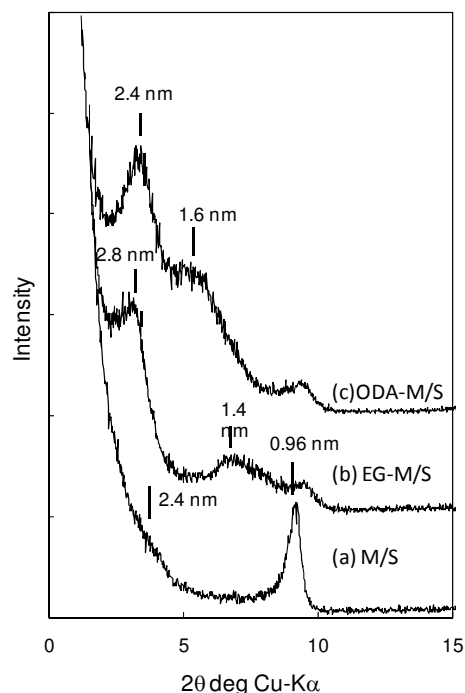


Fig. 7. XRD patterns of (a) product (I), (b) ethylene glycol-treated product (I) (EG-MS), and (c) ODA-modified product (I). XRD data were collected using Cu-K $\alpha$  radiation.

$2\theta = 3.6^\circ$ , corresponding to 2.4 nm. After treatment with EG, the 001 reflection shifted to a lower angle, from 2.4 nm to 2.8 nm and a 002 reflection appeared. Curve (c) is the XRD pattern of the ODA treated sample. Three broad reflections at 2.4 nm, 1.6 nm, and 0.94 nm were observed, which correspond to the 002, 003 and mica phases, respectively. The basal spacing of the ODA-product (I) is estimated to be 4.8 nm. All XRD results indicate that the layer structure is a 1:1 regularly interstratified structure consisting of the mica/smectite sequence we refer to as M/S. This is a “Rectorite-like type interstratified silicate” (Fig. 8).

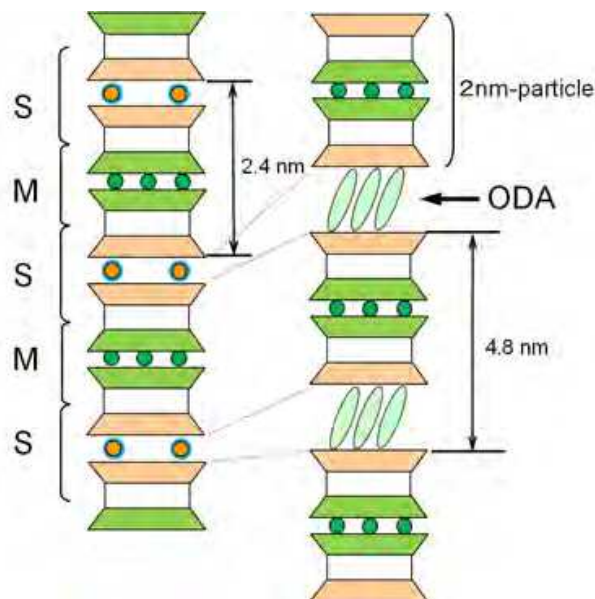


Fig. 8. Schematics of (left) product (I); orderly interstratified mica/smectites (M/S) and (right) ODA-M/S structures.

**Product (II)** By hydrothermal treatment of quenched glass with composition (II) at 450°C for 20 days, a regularly interstratified structure was recognized (Tamura et al., 2009). The pristine product shows three broad reflections of 2.7 nm, 1.35 nm and 1 nm, respectively (Fig. 9, curve (a)). For the EG treated sample, curve (b), two reflections shift to lower angles. These correspond to 001, and 002, respectively (curve (b)). The line profiles suggest that the layer structure of product (II) is a 1:1 regularly interstratified structure consisting of the chlorite(C)/smectite (S) sequence we refer to as C/S. Thus, we have a “corrensite”-like interstratified silicate (Fig. 10). Curve (c) in Fig. 9 is an XRD pattern of the ODA treated sample. Two broad reflections of 3.2 nm and 1.6 nm were observed, which correspond to the 001 and 002 reflections, respectively.

**Product (III)** By hydrothermal treatment of quenched glass with composition (III) at 350°C for 7 to 21 days, a unique regularly interstratified clay mineral composed of talc/talc/smectite (T/T/S) was recognized (Tamura et al., 2008). For the pristine product, three broad reflections of 3.5 nm, 1.7 nm, and 1.0 nm were observed, which correspond to the 001, 002, and 003 reflections, respectively (Fig. 11, curve (a)). After treatment with EG, all three reflections shifted to lower angles of 3.7 nm, 1.8 nm, and 1.2 nm (Fig. 11, curve (b)). These results suggest that the layer structure of product (III) is a 2:1 regularly interstratified structure consisting of the talc/talc/smectite sequence that we call T/T/S (Reichweite ordering parameter: R2). This is a new regularly interstratified clay mineral in an ordered sequence.

The  $d_{001}$  phase at 5.2 nm is a super-lattice of the compound formed by the intercalation of ODA<sup>+</sup> molecules (Fig. 11, curve(c)). Figure 12 schematically depicts the ordered interstratified T/T/S and organically modified T/T/S (ODA-T/T/S) structures.

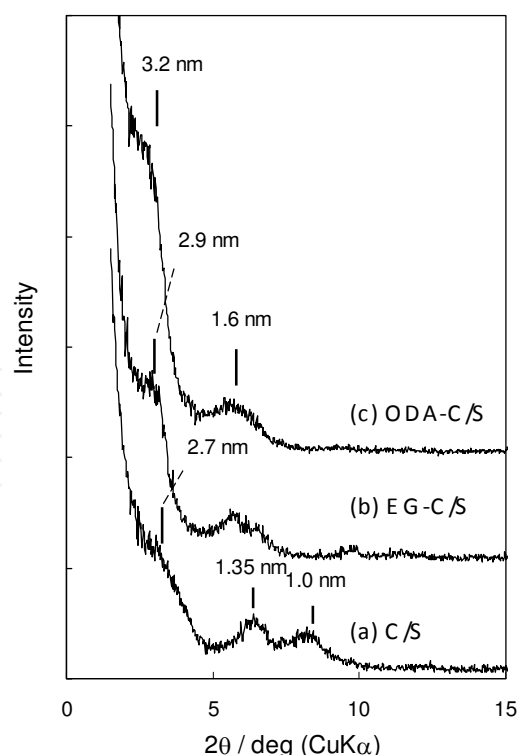


Fig. 9. XRD patterns of (a) product (II), (b) ethylene glycol-treated product (II) (EG-C/S), and (c) ODA-modified product (II). XRD data were collected using Cu-K $\alpha$  radiation.

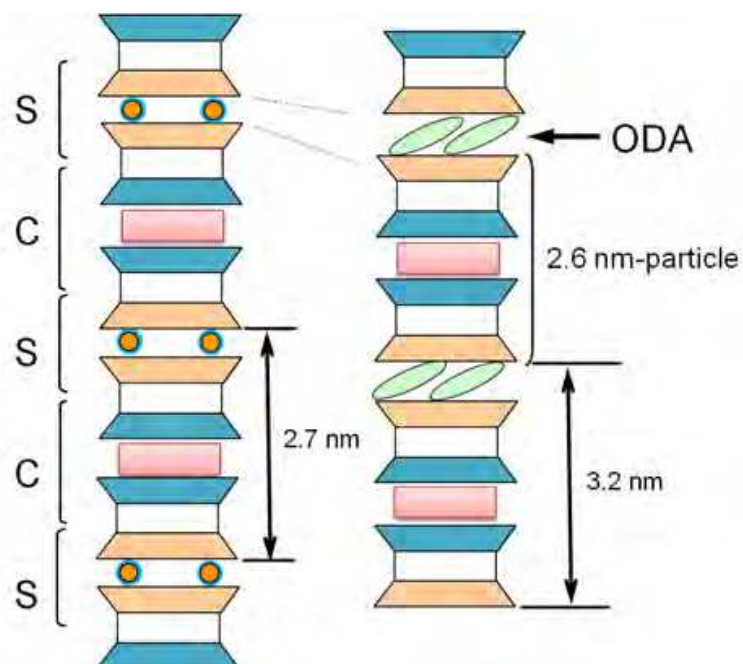


Fig. 10. Schematics of (left) product (II); orderly interstratified chlorite/smectites (C/S) and (right) ODA-C/S structures.

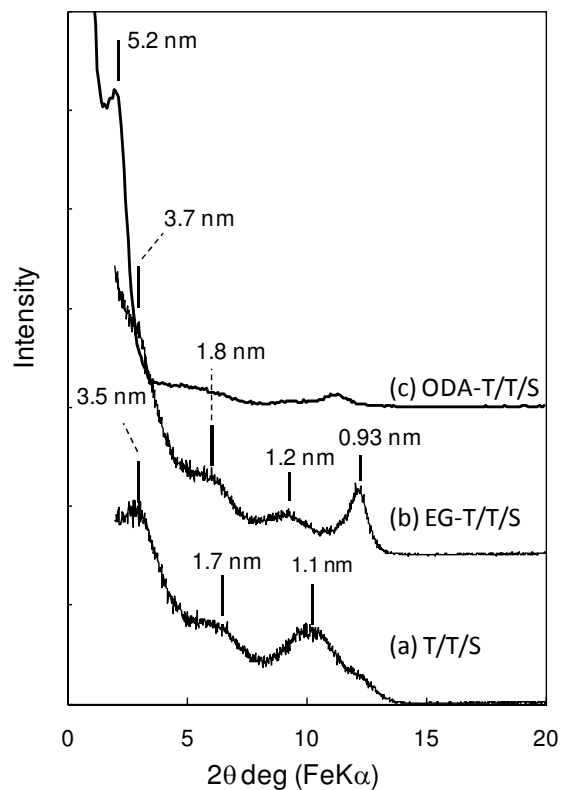


Fig. 11. XRD patterns of (a) product (III), (b) ethylene glycol-treated product (III) (EG-T/T/S), and (c) ODA-modified product (III). XRD data were collected using Fe-K $\alpha$  radiation.

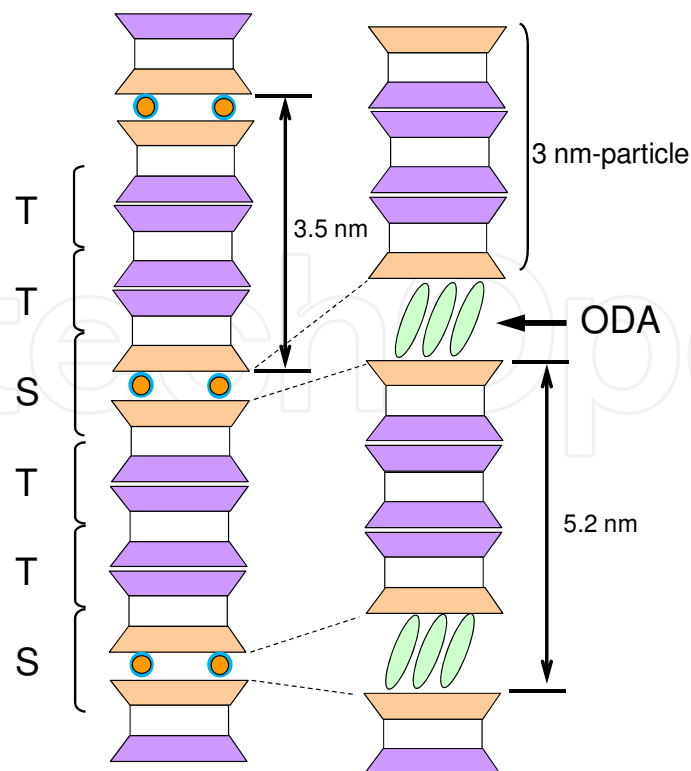


Fig. 12. Schematics of (left) product (III); orderly interstratified talc/talc/smectites (T/T/S) and (right) ODA-T/T/S structures.

#### 4.2.3 Preparation of nanocomposite

The ODA-modified silicate powder was added to diglycidyl ether of bisphenol A (DGEBA) and cured with methyl nadic anhydride (MNA). Benzyl dimethylamine (BDMA) was used as a catalyst. Samples were cured at 150°C for 6 h.

Figure 13 shows transmission electron microscopy (TEM) images of (a) [ODA-M/S]-epoxy, (b) [ODA-C/S]-epoxy, and (c) [ODA-T/T/S]-epoxy, respectively. The dark areas represent the silicate layers and the gray/white areas represent the epoxy matrix. It would seem that the dispersed platelets (units) are thicker than those of a completely exfoliated (monolayer dispersed) clay-polymer nanocomposite. In the TEM image of the [ODA-M/S]-epoxy composite, partially exfoliated double layers (2-nanolayer/group) can be seen (Fig. 13a). In the [ODA-C/S]-epoxy composite, flocculated silicate layers ranging from about 50 nm to 200 nm in thickness were observed (Fig. 13b). It seems, however, that fine particles might be partially exfoliated in the epoxy matrix. Closer observation of the nanocomposite at high magnification confirms a rather rigid platelet (cross section), in which the length of the cross section is a few hundred nanometers and its thickness is approximately 3 nm. Most of the nanolayers appear to be 3 layers per unit (C/S: the thickness is a ca. 2.5 nm).

The [ODA-T/T/S]-epoxy nanocomposite has an especially homogeneous dispersion of ODA-TTS platelets in the epoxy matrix (Fig. 13c). The TEM image confirms a rather rigid platelet (cross section), in which the length of the cross section is a few hundred nanometers and it is approximately 3 nm to 5 nm thick. Most of the dispersed nanolayers shown in Fig. 13c are actually 3 nanolayers grouped together. The 3-layer group thickness of approximately 5 nm, deduced from the TEM images, is thicker than that of the 3 silicate layers (minimum thickness

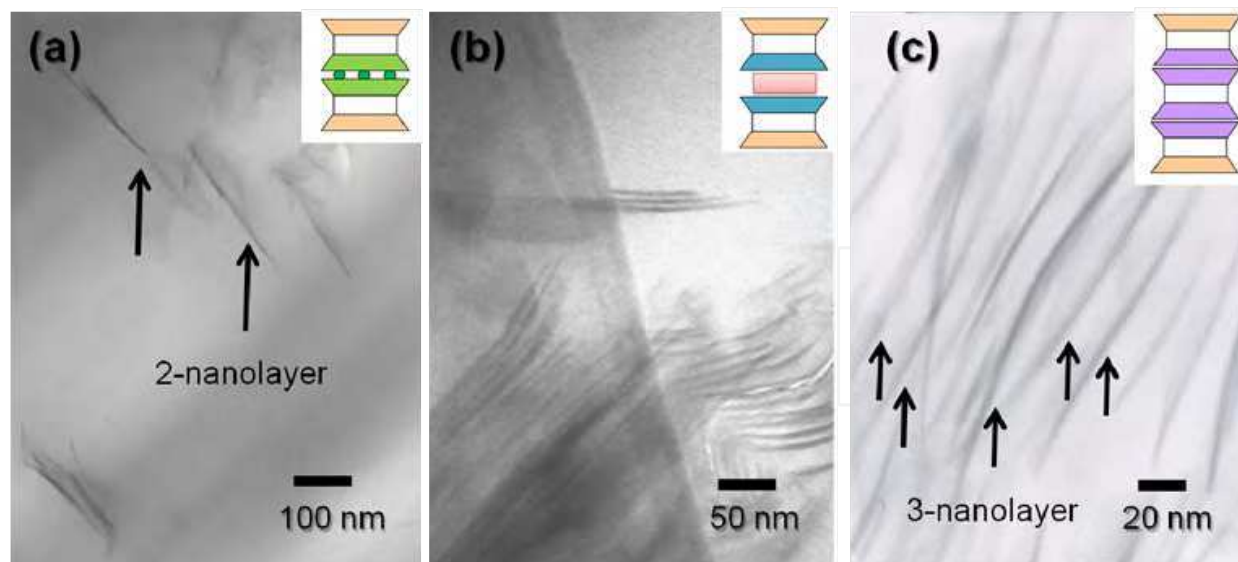


Fig. 13. TEM images of thin sections of glassy epoxy composites cured at 150°C for 6 h: (a) [ODA-M/S]-epoxy system, (b) [ODA-C/S]-epoxy system, (c) [ODA-T/T/S]-epoxy nanocomposite. The weight fraction of each loading was 2.5% silicate. The insets show supposed unit layers .

of about 3.5 nm) that could be caused by the tilting of layers that are inclined obliquely to the sectioned plane. Despite the thicker dimension, the image clearly shows that perfect exfoliation of a 3-layer unit (T/T/S) has taken place, showing that we succeeded in dispersing silicate nanolayers consisting of several layers in one group in a polymer.

## 5. Summary

Following the pioneering work of Toyota researchers who demonstrated the first practical application of a clay-nylon 6 nanocomposite in the automobile industry (Kurauchi et al., 1991), numerous researchers have reported the preparation of exfoliated clay-polymer nanocomposites in various polymer systems. A range of factors that influence not only the morphology but also the final properties of composites have been identified, including the nature of the polymer, the nature of the clay minerals, interfacial interactions between the clay minerals and the polymer, the processing methodologies, and the amount of clay. In order to optimize the properties of nanocomposites so that they can be used effectively in practical applications, we need to take a comprehensive view of all these factors when designing the material. We strongly believe that broadening our scope in order to utilize various types of clay minerals and methods will be essential to achieve that goal.

In this chapter, several examples of polymer nanocomposites using different types of regularly interstratified clay minerals have been introduced. Generally, smectites and other expandable layered silicates are versatile materials that, in a practical sense, are well adapted to yield a large variety of nanocomposites due to their ion exchange, expandability, and colloidal properties. On the other hand, no one has attempted to use regularly interstratified clay minerals, the so-called “mixed clay minerals”, despite their unique structure of highly ordered silicate nanolayers (an ordered sequence along the  $c^*$  direction)

to create new nanocomposites due to their unavailability and metastability. Peculiar clay minerals could potentially extend the field of high performance materials beyond traditional applications to encompass new unexpected functions. For the future, to design high-performance nanocomposites, highly precise control of morphology ranging from the microscopic to the macroscopic scale will be probed using various interstratified minerals.

## 6. References

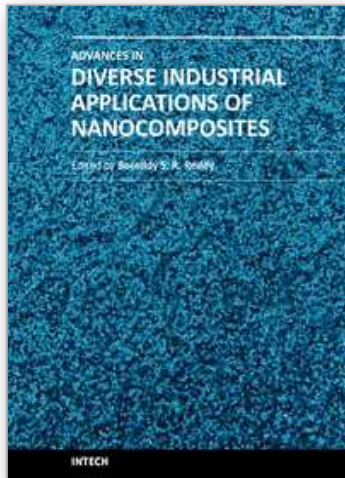
- Altaner, S.P., Weiss, C. A. & Kirkpatrick, R.J., (1988). Evidence from  $^{29}\text{Si}$  NMR for the structure of mixed-layer illite/smectite clay minerals. *Nature*, 331, 699-702.
- Altaner, S. P. & Ylagan, R. F., (1997). Comparison of Structural models of Mixed-Layer Illite-Smectite and reaction Mechanisms of Smectite Illitization. *Clays. Clay. Miner.*, 45, 517-533.
- Barron, R., F., Slade, P. & Frost, R.L., (1985). Solid-state silicon-29 spin-lattice relaxation in several 2:1 phyllosilicate minerals. *J. Phys. Chem.*, 89, 3880-3885.
- Giannelis, E.P. (1992). A New Strategy For Synthesizing Polymer Ceramic Nanocomposites. *JOM*, 44, 28-30.
- Haraguchi, K. & Takehisa, T. (2002). Nanocomposite hydrogels: a unique organic-inorganic network structure with extraordinary mechanical, optical, swelling/de-swelling properties. *Adv. Mater.*, 14, 1120-1124.
- Jagodzinski, H. (1949a). Eindimensionale Fehlordnung in Kristallen und ihr Einfluss auf die Röntgeninterferenzen. I. Berechnung des Fehlordnungsgrades aus den Röntgenintensitäten. *Acta. Cryst.*, 2., 201-207.
- Jagodzinski, H. (1949b). Eindimensionale Fehlordnung in Kristallen und ihr Einfluss auf die Röntgeninterferenzen. II. Berechnung der fehlgeordneten dichtesten Kugelpackungen mit Wechselwirkungen der Reichweite 3. *Acta. Cryst.*, 2., 208-214.
- Jagodzinski, H. (1949c). Eindimensionale Fehlordnung in Kristallen und ihr Einfluss auf die Röntgeninterferenzen. III. Vergleich der Berechnungen mit experimentellen Ergebnissen. *Acta. Cryst.*, 2., 298-304.
- Jakobsen, H.J., Neilsen, N. C. & Lindgreen, H. (1995). Sequences of Charged Sheets in Rectorite. *Am. Mineral.*, 80, 247-252.
- Kurauchi, T., Okada, A., Nomura, T., Nishio, T., Saegusa, S. & Deguchi, R. (1991). Nylon 6-Clay Hybrid-Synthesis, Properties and Application to Automotive Timing Belt Cover. *SAE Technical Paper*, 910584, 1-7.
- Maiti, P., Yamada, K., Okamoto, M., Ueda, K. & Okamoto, K. (2002). New polylactide /layered silicate nanocomposites: Role of organoclays. *Chem. Mater.*, 14, 4654-4661.
- Messersmith, P.B. & Giannelis, E.P. (1994). Synthesis and characterization of layered silicate-epoxy nanocomposites. *Chem. Mater.*, 6, 1719-1725.
- Murakami, T., Inoue, A., Lanson, B., Meunier, A., Beaufort, D. (2005). Illite-smectite mixed-layer minerals in the hydrothermal alteration of volcanic rocks: II. One-dimensional HRTEM structure images and formation mechanisms. *Clays. Clay. Miner.*, 53, 440-451.
- Nadeau, P. H., Tait, J. M. McHardy, W. J. & Wilson, M. J. (1984). Interstratified XRD Characteristics of Physical Mixtures of Elementary Clay Particles. *Clay. Miner.*, 19, 67-76.

- Nagase, T., Ebina, T., Torii, K., Iwasaki, T., Hayashi, H., Onodera, Y. & M. Chatterjee, M. (2000). TEM Observation of Interstratified Ni-Serpentine/Smectite Compounds. *Chem. Lett.*, 344-345.
- Olives, J., Amouric, M., Perbost, R. (2000). Mixed Layering of Illite-Smectites: Results from High-Resolution Transmission Electron Microscopy. *Clay. Clay. Miner.*, 48, 282-289.
- Plançon, A., (2004). Consistent Modeling of the XRD Patterns of Mixed-Layer Phyllosilicates. *Clays. Clay. Miner.*, 52, 47-54.
- Reynolds, R. C. (1980). Interstratified Clay Minerals, In: *Crystal Structures of Clay Minerals and Their X-ray Identification*, Brindley, G. W. & Brown, G., (Ed.), 249-303, Mineralogical Society, London.
- Stixrude, L. & Peacor, D. R., (2002) First-Principles Study of Illite-Smectite and Implications for Clay Mineral Systems. *Nature*, 420, 165-168.
- Suzuki, M., Ohashi, F., Inukai, K., Maeda, M., Tomura, S. & Mizota, T. (2001). Hydration enthalpy measurement and evaluation as heat exchangers of allophane and imogolite. *J. Ceram. Soc. Jpn.*, 109, 681-685.
- S'rodon, J. & Eberl, D. D. (1984). Illite, In: *Micas, Vol. 13 in Reviews in Mineralogy*, Bailey, S. W., (ed), 495-544, Mineralogical Society of America, Washington, D.C.
- Tamura, K. & Nakazawa, H. (1996). Intercalation of n-alkyltrimethylammonium into swelling fluoro-mica. *Clays. Clay. Miner.*, 44, 501-505.
- Tamura, K., Yamada, H. & Nakazawa, H. (2000) Stepwise hydration of high-quality synthetic smectite with various cations. *Clays. Clay. Miner.*, 48, 400-404.
- Tamura, K., Sasaki, T., Yamada, H. & Nakazawa, H. (1999). Laue function analysis of colloidal lithium taeniolite. *Langmuir*, 15, 5509-5512.
- Tamura, K., Yamada, H., Yokoyama, S. & Kurashima, K. (2008). Regularly Interstratified Layered Silicate-Polymer Nanocomposite, *J. Am. Ceram. Soc.*, 91, 3668-3672.
- Tamura, K., Yamada, H., Yokoyama, S., Kurashima, K. (2009). *Abstracts of 14<sup>th</sup> International Clay Conference (ICC 2009)*, pp , Preparation of Regularly Interstratified Layered Silicate-Polymer Nanocomposite. Castellaneta Marina (Italy), June, 2009.
- Torii, K., Onodera, Y., Hayashi, H., Nagase, T. & Iwasaki, T. (1998). Hydrothermal Synthesis of Interstratified Lizardite/Saponite. *J. Am. Ceram. Soc.*, 81, 447-449.
- Usuki, A., Kawasumi, M., Kojima, Y., Fukushima, Y., Okada, A., Kurauchi, T. & Kamigaito, O. (1993). Synthesis of Nylon 6-Clay Hybrid. *J. Mater. Res.*, 8, 1179-1184.
- van Olphen, H. (1977). Clay Mineralogy, In: *An introduction to clay colloid chemistry: for clay technologists, geologists, and soil scientists.*, 57-82, John Wiley & Sons Inc., New York.
- Wang, Z. & Pinnavaia, T.J. (1998). Nanolayer reinforcement of elastomeric polyurethane. *Chem. Mater.*, 10, 3769-3771.
- Yamada, H., Yoshioka, K., Tamura, K., Fujii, K. & Nakazawa, H. (1999). Compositional gap in dioctahedral-trioctahedral smectite system: beidellite-saponite pseudo-binary join. *Clays. Clay. Miner.*, 47, 803-810.
- Yamada, H., Tamura, K., Morimoto, K., Yokoyama, S. & Hatta, T. (2010). *Abstracts of Mid European Clay Conference (MECC2010)*, pp. -, Synthesis and Characterization of Phyllosilicates in Montmorillonite - Stevensite Compositional Series. Budapest (Hungary), Aug, 2010.

Yano, K. Usuki, A. & Okada, A. (1997). Synthesis and Properties of Polyimide-Clay Hybrid Films. *J. Polym. Sci. A. Polym. Chem.*, 35, 2289-2294.

IntechOpen

IntechOpen



## **Advances in Diverse Industrial Applications of Nanocomposites**

Edited by Dr. Boreddy Reddy

ISBN 978-953-307-202-9

Hard cover, 550 pages

**Publisher** InTech

**Published online** 22, March, 2011

**Published in print edition** March, 2011

Nanocomposites are attractive to researchers both from practical and theoretical point of view because of combination of special properties. Many efforts have been made in the last two decades using novel nanotechnology and nanoscience knowledge in order to get nanomaterials with determined functionality. This book focuses on polymer nanocomposites and their possible divergent applications. There has been enormous interest in the commercialization of nanocomposites for a variety of applications, and a number of these applications can already be found in industry. This book comprehensively deals with the divergent applications of nanocomposites comprising of 22 chapters.

### **How to reference**

In order to correctly reference this scholarly work, feel free to copy and paste the following:

Kenji Tamura and Hirohisa Yamada (2011). Morphology Development of Polymer Nanocomposites: Utilizing Interstratified Clay Minerals from Natural Systems, *Advances in Diverse Industrial Applications of Nanocomposites*, Dr. Boreddy Reddy (Ed.), ISBN: 978-953-307-202-9, InTech, Available from: <http://www.intechopen.com/books/advances-in-diverse-industrial-applications-of-nanocomposites/morphology-development-of-polymer-nanocomposites-utilizing-interstratified-clay-minerals-from-natura>

**INTECH**  
open science | open minds

### **InTech Europe**

University Campus STeP Ri  
Slavka Krautzeka 83/A  
51000 Rijeka, Croatia  
Phone: +385 (51) 770 447  
Fax: +385 (51) 686 166  
[www.intechopen.com](http://www.intechopen.com)

### **InTech China**

Unit 405, Office Block, Hotel Equatorial Shanghai  
No.65, Yan An Road (West), Shanghai, 200040, China  
中国上海市延安西路65号上海国际贵都大饭店办公楼405单元  
Phone: +86-21-62489820  
Fax: +86-21-62489821

© 2011 The Author(s). Licensee IntechOpen. This chapter is distributed under the terms of the [Creative Commons Attribution-NonCommercial-ShareAlike-3.0 License](#), which permits use, distribution and reproduction for non-commercial purposes, provided the original is properly cited and derivative works building on this content are distributed under the same license.

IntechOpen

IntechOpen